

Incandescence-based single-particle method for black carbon quantification in lake sediment cores

N. J. Chellman ^{1,2,*} J. R. McConnell,¹ A. Heyvaert,¹ B. Vannière,³ M. M. Arienzo,¹ V. Wennrich⁴

¹Division of Hydrologic Sciences, Desert Research Institute, Reno, Nevada

²Graduate Program of Hydrologic Sciences, University of Nevada, Reno, Nevada

³UMR Chrono-Environnement, CNRS, University Bourgogne Franche-Comté, Besançon, France

⁴Institute of Geology and Mineralogy, University of Cologne, Köln, Germany

Abstract

Refractory black carbon (rBC) is an important contributor to radiative forcing, so quantifying rBC emissions and transport is critical for accurate climate modeling. Formed during incomplete combustion of fossil fuels or biofuels, rBC is emitted to the atmosphere from large wildfires and industrial sources where it can be transported and deposited globally. Ice cores have been used to reconstruct historical changes in biomass burning and industrial emissions but they are available only from glaciers and ice sheets, with reliable records longer than a few centuries generally limited to polar regions. Lake sediment cores provide a possible alternative to develop longer term, widely distributed records from mid- and low-latitude regions, albeit with lower temporal resolution and less directly linked to atmospheric concentrations than ice-core rBC records. Here, we present a new incandescence-based method for measuring rBC in lake sediment cores using the Single-Particle Soot Photometer. Compared to existing filter-based techniques, this highly sensitive method requires a much smaller sample size, resulting in reproducible, relatively high-temporal-resolution records of past rBC deposition.

Black carbon (BC) is produced from incomplete combustion and can refer to a spectrum of materials affected by combustion ranging from fragments of slightly burned organic material up to 100 μm in size to submicron, condensed soot. In this article, we refer to the most condensed, submicron soot BC particles, commonly referred to as refractory BC (rBC) (Petzold et al. 2013). rBC is an unambiguous tracer of biomass combustion during the preindustrial, and a tracer of biomass, coal, and oil combustion after industrialization. rBC records from ice cores (McConnell et al. 2007; McConnell and Edwards 2008; Bisiaux et al. 2012, 2012; Bauer et al. 2013; Painter et al. 2013; Keegan et al. 2014; Zennaro et al. 2014; Arienzo et al. 2017; Chellman et al. 2017), snow (Schwarz et al. 2013; MacDonald et al. 2017), and lake sediments (Gustafsson et al. 2001; Muri et al. 2002; Louchouart et al. 2007; Khan et al. 2009; Han et al. 2011; Ruppel et al. 2015) have been used extensively as proxies for historical burning emissions. The BC aerosol is important not only as a conservative tracer of historical fire activity but also because of its impact on radiative forcing. When deposited on bright surfaces such as snow, small amounts of rBC can darken snow, reduce its albedo, and enhance melt (McConnell et al. 2007; Bond et al. 2013; Painter et al. 2013). However, ice-core records in the Arctic (i.e., the NEEM ice core [Dahl-Jensen et al. 2013]) and Antarctic

(i.e., the Dome Concordia ice core [Augustin et al. 2004]) are limited to the past 130 and 800 kyr, respectively. Furthermore, well-dated ice-core records longer than a few centuries generally can be recovered only from the polar regions at sites located far from extensive low- and mid-latitude rBC source regions.

As an alternative, lake-sediment cores are not geographically restricted to the polar regions and potentially provide much longer biomass burning records, in some cases, spanning multiple glacial/interglacial climate cycles (Melles et al. 2012; Brigham-Grette et al. 2013). Charcoal measurements in lake-sediment cores routinely are used to develop records of past fire activity, but because each charcoal record reflects burning only in the area within tens of kilometers of the lake (Whitlock and Millsaugh 1996; Marlon et al. 2008; Vannière et al. 2008), many individual charcoal records must be combined to estimate a larger-scale regional fire history. Sub-micron rBC particles, as quantified by the method presented here, are approximately three orders of magnitude smaller than charcoal fragments and transported through eolian rather than fluvial processes, so rBC records implicitly reflect regional-scale or even continental-scale emissions (Vannière et al. 2011; Vannière et al. 2016).

Previous methods to measure BC in lake sediment cores have largely been limited to (1) filter-based thermal-optical and (2) chemothermal oxidation methods. Thermal/optical

*Correspondence: nathan.chellman@dri.edu

transmittance and reflectance methods (TOT/R) have been used extensively for monitoring atmospheric aerosol organic and BC content, though when adapted to soil and sediment studies were susceptible to strong interferences from nonpyrogenic carbon. The chemothermal oxidation method (CTO-375) has been shown to be sensitive to soot in sediment and soil samples and has a low sample requirement of ~ 10 mg. While effective at measuring a wide range of the BC continuum, some of the filter-based methods require large sample sizes that limit resolution or time-consuming analytical methods such as chemical pretreatment. Furthermore, they can be hampered by measurement artifacts such as uncertainties associated with carbon volatility and interferences during thermal evolution of the sample resulting from either charring of organic materials or nonpyrogenic carbon present in certain matrices such as coal or shale (Gustafsson et al. 2001; Muri et al. 2002; Yang and Yu 2002; Hammes et al. 2007; Louchouart et al. 2007; Khan et al. 2009; Han et al. 2011; Ruppel et al. 2015).

Here, we present a new method for measuring rBC in lake sediment cores based on the Single-Particle Soot Photometer (SP2; Droplet Measurement Technologies [DMT]), an instrument that has been used extensively for measurements of rBC in atmospheric aerosols (Schwarz et al. 2006; Moteki et al. 2007; Subramanian et al. 2010), as well as in rainwater (Ohata et al. 2013), snow (Schwarz et al. 2013), and ice cores (McConnell et al. 2007; McConnell and Edwards 2008; Arienzo et al. 2017). These and other studies have documented that the SP2 is sensitive to submicron, highly condensed soot produced by combustion of diesel, wood, or laboratory-generated soot and for soot-dominated atmospheric samples, SP2 measurements are directly comparable to measurements made with TOT/R methods (Kondo et al. 2011; Laborde et al. 2013).

The procedure detailed here was adapted from a method developed for ice cores first established by McConnell et al. (2007) that uses a nebulizer to transform an aqueous sample into a dry aerosol which subsequently is analyzed by the SP2 via laser-induced incandescence of rBC. With this new lake-sediment method, highly reproducible rBC measurements can be made with as little as 15 mg of sediment (although 50 mg is preferred), permitting high-resolution records. Sample preparation times are short, leading to high sample throughput with the ability to analyze up to 70 samples per day.

Materials and procedures

Preparation of lake sediment samples

Lake sediment samples were resuspended into an aqueous solution prior to introduction into the nebulizer/SP2 system. Lake sediment samples from Lake El'Gygytgyn (eastern Siberia, Russia [Melles et al. 2007; Brigham-Grette et al. 2013]) and Island Lake (Beartooth Pass, Wyoming) were used in this study. Sediment samples were dried and homogenized for 3 min for Lake

El'Gygytgyn samples and 5 min for Island Lake samples using a planetary mill (Pulverisette 5, Fritsch) with an agate grinding bowl and agate grinding balls. Samples were stored in plastic vials or zip lock bags until analysis. Approximately 50 mg of dried and homogenized lake sediment was suspended in 50 mL of ultrapure 18.2 M Ω water in a precleaned and dry polypropylene vial. Sediment samples were not chemically pretreated. The weight of both the sediment and water was used to determine the exact ratio of sediment mass to water volume in units of milligrams of dry sediment per milliliters of water. This ratio allowed for normalization of the measured rBC concentration to obtain a final determination of nanograms of rBC per milligram sediment. Replicate samples were prepared to ensure day-to-day agreement between measurements.

After a batch of samples was suspended in water, the samples were sonicated for 7.5 min (B8510MT Ultrasonic Cleaner; Emerson Electric), shaken vigorously by hand to remobilize settled sediment, and immediately sonicated for another 7.5 min with the goal of mobilizing rBC from the sediment matrix. The samples were then placed on a platform shaker (New Brunswick Innova 2100; Eppendorf, Hamburg, Germany) for 16 h, after which the samples were sonicated for 30 min and again shaken vigorously by hand halfway through sonication. Prior to analysis, samples were stored in a refrigerator at 10°C for 24 h under the assumption that the less-dense, submicron rBC particles will remain in aqueous solution while larger, denser sediment particles that may clog the nebulizer or contaminate the SP2 optics will settle out of solution.

Liquid samples were introduced continuously to the analytical system using an autosampler (ASX510; Teledyne Cetac) and peristaltic pump (Fig. 1). All aqueous sample delivery lines were Teflon™. The high sediment load and high concentration of rBC in lake sediment cores, compared to similar analysis in ice and snow, require coarse-particle filtering and dilution to prevent contamination or clogging of the analytical system and SP2 optics. Particle filtration of the aqueous sample and all suspended constituents was accomplished by sequential 20 and 10 μ m stainless steel inline filters, which have large enough pores to let rBC particles pass unimpeded but will remove larger sediment particles. Undiluted sample first was pumped from the autosampler through the inline filters to a debubbler constructed from a 1 mL pipet tip, after which the ultrapure water was added to dilute the bubble-free

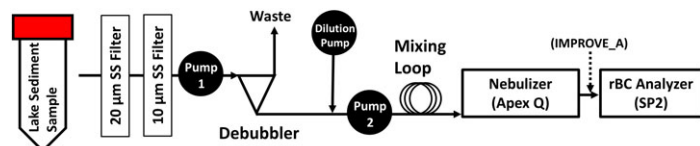


Fig. 1. Schematic of the sample introduction system for lake sediment samples. Dashed arrow denoted by (IMPROVE_A) indicates where a quartz fiber filter was inserted to capture aerosol for independent method verification.

sample using a precision pump. With a total flow of 600 $\mu\text{L}/\text{min}$ required for aerosol generation by the Apex-Q nebulizer, inline dilution flows ranged from 300 to 500 $\mu\text{L}/\text{min}$ resulting in dilution ratios ranging from 1 : 1 to 1 : 5. Dilution ratios were kept constant for the entire measurement campaign, including for calibration and quality control standards. An inline mixing loop made from coiled ~ 1 m length of 0.25 mm ID Teflon™ tubing was used to ensure complete mixing of the sample and dilution flow streams. The diluted sample was delivered via peristaltic pump (Ismatec, Cole-Parmer) to the Apex-Q nebulizer to transform the aqueous flow into a dry aerosol which was then analyzed by the SP2 (Fig. 1).

SP2 and nebulizer system

rBC measurements using the SP2 require a sample stream of dry aerosol. To generate a dry aerosol from a suspended sediment sample, this new method uses a jet-type nebulizer (Apex-Q; Elemental Scientific) which has been shown to be more efficient over a wide size range of particles compared to ultrasonic nebulizers (Wendl et al. 2014). The dry aerosol is passed via conductive silicone tubing from the nebulizer into the SP2's cavity where a 1064-nm Nd : YAG laser heats individual rBC particles to their boiling point. The radiation produced by the incandescent rBC particles is measured by two photomultiplier tubes with different gain settings, each measuring over both narrowband and broadband wavelength ranges. The peak intensity of the incandescence is directly proportional to each rBC particle's mass, and the ratio of the narrowband and broadband peak heights, known as the color ratio, can be used to evaluate interferences from any non-rBC particles. The instrument's response is much more sensitive to rBC than dust or organic material (Schwarz et al. 2013; Yoshida et al. 2016), so it generally is not necessary to pretreat atmospheric or snow and ice samples to isolate rBC. The SP2 laser power, as indicated by the YAG power parameter on the instrument, was kept above 3 V to ensure sufficient incandescence.

Two calibration steps were used to obtain final rBC mass concentrations and mass distributions, the first to calibrate the internal SP2 response and the second largely to adjust for efficiency of the sample introduction system. First, an internal calibration relates the peak incandescence signal to a rBC mass for each particle detected by the SP2. The SP2 used in this study was calibrated with the manufacturer-specified procedure using a differential mobility analyzer up to a rBC mass of 60 fg using the rBC-like material Aquadag, a colloidal suspension of graphite with a well-quantified effective density (Gysel et al. 2011). This nearly linear calibration curve was extrapolated to 100 fg. For more information on SP2 calibration and mechanics, see Schwarz et al. (2010), Gysel et al. (2011), Baumgardner et al. (2012), and Laborde et al. (2012). Lognormal distributions fit to particle mass distributions and their corresponding cumulative distribution functions indicated that this mass range captures > 95% of the rBC in typical lake-sediment samples. SP2 data were processed using the Probe

Analysis Package for Igor software provided by DMT. Particles with color ratios (calculated as the log base 10 of the ratio of the broadband to narrowband peak heights) outside of the optimum rBC range between -0.15 and 0.2 were removed, the remaining single-particle measurements were transformed from incandescence to mass, and rBC mass concentrations were calculated by accumulating single-particle data into three-second bins.

Second, aqueous standards made from two rBC-like standard materials of known concentration were run through the entire analytical system as an external calibration to account for nebulization efficiency and drift. A full-suite of standards run at the beginning of each day was used to calibrate the analytical system for rBC concentration, and quality control standards were measured throughout each analysis day and used to correct for drift. Standards were made from (1) Cabojet 200, assuming a rBC content of 88% (Wendl et al. 2014), and (2) Aquadag, assuming a rBC content of 76% (Gysel et al. 2011). We used Cabojet 200, which has a particle size distribution ranging from 0.1 to 3 fg (~ 50 to 150 nm volume equivalent diameter), because of its long-term stability, permitting confidence in measurements made years apart, and Aquadag, which has a particle size distribution ranging from 0.1 to 100 fg (Fig. 2a; ~ 50 to 500 nm volume equivalent diameter), because it has the largest mass distribution of any commonly-used rBC-like standard material. Hence, Aquadag is more comparable to the rBC mass distributions observed in lake sediment samples (Fig. 2a) relative to other rBC standard materials that are much smaller (Wendl et al. 2014).

Each lake sediment sample was analyzed for a total of 5 min, with the first 3 min intended to allow the signal to stabilize from the transition between samples and the final 2 min averaged for final rBC values. Typical relative standard error of the mean concentration during the 2-min measurement period was < 1% ($n = 616$). To ensure consistent flow, peristaltic pump tubes were changed weekly. Based on data from 16 analysis days, we estimated a drift of $12\% \pm 5\%$ ($\pm 1\sigma$) over the course of a typical 8- to 10-h analysis run based on quality control standards. Drift was measured during each experiment and the sample measurements adjusted accordingly as part of post-processing. Blanks typically had an average rBC concentration of 0.96 ± 0.70 ng/g ($\pm 1\sigma$, $n = 12$), yielding a detection limit of 2.1 ng/g defined as three times the standard deviation of the blank.

Because the SP2 directly measures rBC mass, we report rBC mass distributions rather than size distributions because the latter requires assumptions of an effective density and a spherical or other shape for rBC particles. When required for comparisons to previous studies, rBC particle mass was converted to size assuming a spherical morphology and a density of 1.8 g/cm³.

Assessment and discussion

To evaluate the new method for rBC measurements in lake sediments, we investigated: (1) potential sediment and matrix

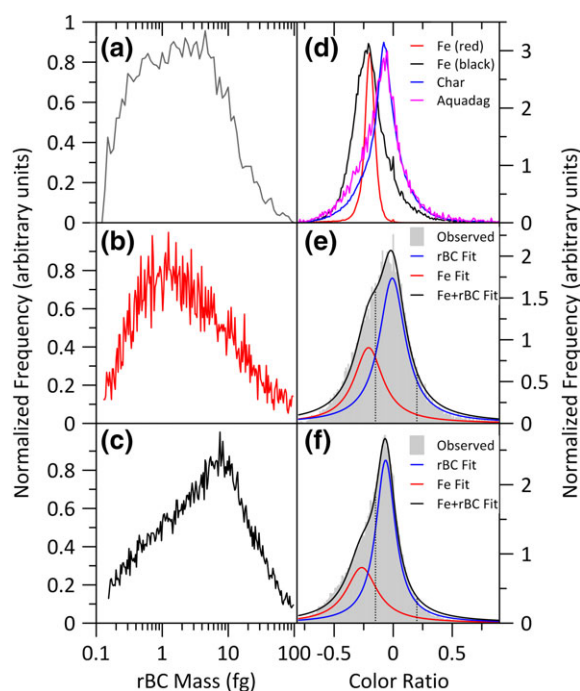


Fig. 2. rBC mass distribution for Aquadag (a), Island Lake (b), and Lake El'Gygytyn (c) samples using equal-width bins in log-space with 20 μm inline filter. Mass distributions are comparable to those reported for rBC in mid-latitude snow and rainwater (Ohata et al. 2013; Schwarz et al. 2013; Wendl et al. 2014) and remained unchanged using 10 and 2 μm inline filters. Color ratios for rBC (Aquadag, char) and iron oxide (i.e., hematite) reference materials (d). Observed (gray) and fit (black) color ratios for Island Lake (e) and Lake El'Gygytyn (f). Fit was calculated as the sum of Cauchy distributions for rBC (blue) and interference (red) portions of the observed color ratio. Only particles with color ratios between the dashed vertical lines at -0.15 and 0.2 were kept in post-processing and used for mass concentration calculations.

interferences, (2) sample stability, (3) rBC recovery, and (4) measurement reproducibility. As a final validation, we also compared lake sediment rBC measurements made using the new SP2-based method to those made using a well-established thermal/optical filter technique previously used for BC measurements in lake-sediment samples (Chow et al. 2007; Han et al. 2007).

Sediment and matrix interferences

Because both rBC and sediment are resuspended as part of this new SP2-based lake-sediment method, we evaluated potential sediment and matrix interferences on the rBC measurements using two approaches.

First, to prevent clogging of the Teflon™ flow lines and to reduce the amount of sediment injected the SP2, the aqueous sample routinely is filtered en route to the nebulizer using two sequential inline stainless steel honeycomb filters, with the first generally a 20 μm filter (Fig. 1). To evaluate potential sediment interferences, we used three different filters (20, 10, and 2 μm) in the second inline filter position and compared measured rBC

concentrations and mass distributions. Because the upper limit of the SP2 calibration in this study was 100 fg corresponding to a volume-equivalent rBC diameter of $\sim 0.47 \mu\text{m}$, rBC will pass unimpeded through filters with pore sizes $> 0.5 \mu\text{m}$. As expected, rBC mass distributions and concentrations remained unchanged for all filters (rBC mass distribution using 20 μm filter shown in Fig. 2b,c), indicating that sediment particles larger than 2 μm were not interfering with SP2-based rBC quantification.

To evaluate potential interferences for particles smaller than 2 μm , we used the color ratio of particles detected by the SP2 to differentiate between interferences and rBC. Iron oxides, specifically hematite and magnetite, are known to interfere with SP2 measurements (Yoshida et al. 2016), and though the SP2 is overall much less sensitive to these interferences, they could be significant contributors for sediment-laden samples. Because iron oxides incandesce at a lower temperature than rBC, the color ratio for iron oxides peaks at about -0.25 , lower than the -0.05 typical for ambient rBC (Fig. 2d) on the SP2 used in this study. Thus, the color ratio can be used to identify and quantify the interference from non-rBC particles.

By fitting two Cauchy distributions to the observed semimodal color ratio for the bulk samples from Island Lake (Fig. 2e) and Lake El'Gygytyn (Fig. 2f), for particles with color ratios between -0.15 and 0.2 kept in post-processing, we estimate the sediment interference to be 20% for Island Lake and 15% for Lake El'Gygytyn in number concentration, corresponding to a total interference of $\sim 15\%$ in mass concentration for both lakes. The range of rBC mass distributions measured in the lake samples were comparable to those reported for rainwater (Ohata et al. 2013), snow (Schwarz et al. 2013; Wendl et al. 2014), and a Mt. Everest ice core (Kaspari et al. 2011), further indicating that sediment interferences were not dominant. For operational purposes, we found the 2 μm filter clogged rapidly so we used a 20 and 10 μm filter in series as standard protocol.

Second, standard addition experiments were performed using samples from Lake El'Gygytyn and Island Lake to assess potential matrix interactions between rBC and the sediment or interferences of the sediment itself on the SP2 measurement (Fig. 3). Standard addition involves spiking samples containing consistent amounts of analyte and matrix (i.e., rBC in sediment) with known and varying amounts of standard material. The concentration of the analyte in solution is predicted by a linear fit to the measured concentration of the spiked samples that is subsequently extrapolated to the x -intercept. No matrix effect is indicated if the standard addition prediction matches the measurement of the sample without standard addition.

Lake sediment samples were spiked with an aqueous Aquadag solution of known concentration immediately after 50 mL of ultrapure water was added to the dry sediment sample, allowing the Aquadag to interact with the suspended sediment matrix through the remainder of the preparation process including sonication and shaking. Four levels of

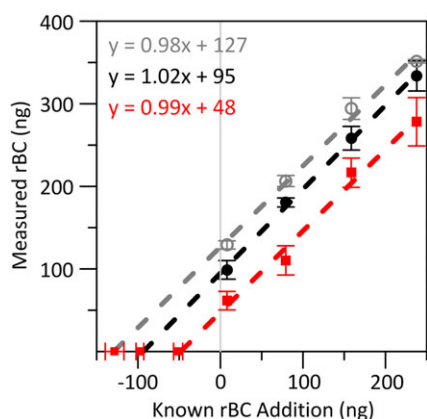


Fig. 3. Standard addition experiments demonstrate no matrix effects. Shown are results for two samples from Lake El'Gygytyn (gray, black) and one sample from Island Lake (red) using the rBC-like material Aquadag as the standard. Red points on the x -axis represent sample measurements without standard addition. Error bars represent $\pm 1\sigma$ ($n = 3$ for all points).

addition with three replicates at each level were performed on each sample, with approximately 3–6 times the rBC concentration of the sediment sample added for the most concentrated addition. We estimated recovery for Aquadag of $97\% \pm 4\%$ ($n = 12$) based on quality control standards. Though Aquadag's graphitic-sheet morphology is different than that of ambient rBC (Moteki et al. 2007), to our knowledge it has the widest mass distribution of any commonly used rBC standard and is more comparable to the rBC mass distributions observed in lake sediment cores (Fig. 2a). It is important for the standard material to have a similar mass distribution as the sample to ensure comparable recovery as controlled by nebulization efficiencies and interactions with the sediment matrix. The linear fit to the spiked samples had a slope of nearly 1, indicating no rotational effects from the matrix on rBC, and the x -intercept of the line matched the measured concentration of the non-spiked samples within the uncertainty of the measurement (Fig. 3).

The results of the filter and standard addition tests confirmed there are no detrimental effects on the rBC measurement from the sediment matrix at Island Lake and Lake El'Gygytyn. However, matrix effects may be present for other lakes with different mineralogy and chemistry so it is recommended that similar tests are completed for analyses of different lakes or, for temporally longer lake sediment cores, during eras with differing depositional environments.

Sample stability

rBC within a sample can be altered by numerous factors including, but not limited to, sedimentation, agglomeration, or adhering to the polypropylene vial, during and after the preparation process. Thus, quantifying the sample's stability through time was necessary to ensure consistent and repeatable results.

To test the stability of the samples through time, a set of four samples was prepared from bulk sediment samples from both Lake El'Gygytyn and from Island Lake. rBC was measured at various intervals between 1 and 55 h after final sonication to quantify the stability of the samples through time up to a maximum settling time of 55 h. Samples were refrigerated between measurements. After 30 h, the concentration decrease for the Island Lake samples was negligible ($1\% \pm 2\%$) and for Lake El'Gygytyn was $9\% \pm 6\%$. After 55 h, rBC concentration decreased by $9\% \pm 2\%$ and $23\% \pm 6\%$ for Island Lake and Lake El'Gygytyn samples, respectively. The rBC color ratio did not change over the course of the experiment suggesting similar settling behavior for rBC and small-particle interferences. The discrepancy in stability between samples from the two lakes could be attributed to different rBC mass distributions, with Lake El'Gygytyn having larger particles (Fig. 2b,c), or sediment chemistry affecting the stability of the aqueous solution.

Ideally, samples would be run immediately after final sonication to avoid changes through time, but this is impractical because of the high suspended sediment load that rapidly clogs the filters, tubing, and nebulizer and also increases the potential to contaminate the SP2 optics, further discussed in the rBC Recovery section below. In light of these issues, we recommend analysis of the samples within the first 30 h of preparation to minimize rBC loss, with a time-dependent, lake-specific correction factor to account for settling.

rBC recovery

To assess overall rBC recovery of the lake sediment samples, BC was measured in sediment samples subjected to four complete preparation cycles, without allowing the samples to settle after final sonication to maximize rBC in suspension. After the first preparation cycle and corresponding rBC measurement, the 50 mL of water and any associated suspended sediment was removed carefully with a pipette, leaving only the settled sediment at the bottom of the conical vial. Fifty milliliter of fresh ultrapure water was added to the settled sediment and the sample was subsequently sonicated, shaken, and reanalyzed. This process was repeated four times. The first measurement represented $58\% \pm 6\%$ ($n = 3$) and $77\% \pm 4\%$ ($n = 5$) of the cumulative total rBC (Fig. 4) for samples made with 50 mg of sediment from Island Lake and Lake El'Gygytyn, respectively. As expected, rBC concentration of the samples subsequently declined with each cycle, and the color ratio did not indicate preferential remobilization of either rBC or interfering sediments. This experiment was repeated with samples prepared with 15 and 25 mg of sediment to test if less sediment loading would increase recovery, but rBC recovery was largely unchanged with the first measurement still representing 60–80% of the cumulative rBC concentration.

Sonication, which uses ultrasonic sound waves to break apart agglomerates, was another potential control on rBC recovery. The goal of sonication in this method is primarily to

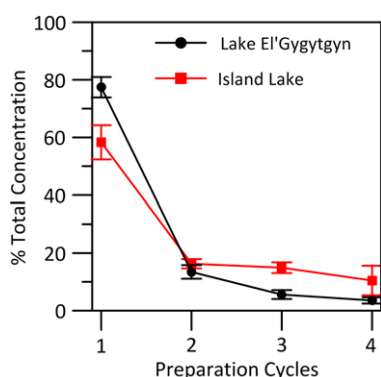


Fig. 4. rBC recovery for Island Lake and Lake El'Gygytgyn samples over four preparation cycles. Measurements from each cycle were accumulated to derive the total concentration. The first measurement represented 60–80% of the total rBC measured for both lakes. Error bars represent $\pm 1\sigma$ ($n = 3$ for all points).

mobilize rBC from the sediment matrix and into aqueous solution without significantly altering the rBC mass distribution. There were two sonication steps during the sample preparation process: a 15-min sonication before shaking the samples overnight for 16 h, and a 30-min sonication after shaking was complete. Here, we tested the duration of the second sonication step, as it occurs after the sediment had been agitated and resuspended by 16 h on the platform shaker. Sonication times of 0, 5, 15, 30, 60, and 120 min were tested on a bulk sample from Lake El'Gygytgyn. Average rBC concentration and mass distributions were unchanged and statistically

indistinguishable at the 95% confidence interval for sonication times of 0, 5, 15, and 30 min. However, the standard deviation of the rBC concentration of samples sonicated for 30 min was lowest of these groups, and the mass distribution was less variable, indicating a more consistent measurement. The rBC concentrations for samples sonicated for 60 and 120 min were 12% and 17% higher than the samples sonicated for 30 min, though the mass distributions for these samples were narrower, indicating the extended sonication time was potentially breaking apart rBC particles or altering the sediment or the polypropylene vial itself. We recommend a 30-min sonication time, similar to the 25-min recommendation for SP2 rBC measurements in snow samples from Wendl et al. (2014).

Reproducibility

This method yields highly reproducible results for both rBC measurements made on a single sample (i.e., measurement replicates) as well for measurements made on replicate samples prepared from the same original sediment (i.e., method replicates). The method and measurement replicates for samples from Lake El'Gygytgyn and Island Lake are shown in Fig. 5. Measurement replicates ensure that samples are not changing significantly during the analysis run. We estimate an average relative percent difference (RPD; calculated as the absolute value of the difference between paired replicate measurements divided by their average) of 8% ($n = 54$) and 4% ($n = 32$) for Lake El'Gygytgyn and Island Lake measurement replicates, respectively, made within an 8-h window. This low error indicates high measurement reproducibility and is consistent with the previously demonstrated stability of the samples. When considering replicate measurements made within a 30-h window, the average RPD for Lake El'Gygytgyn measurement replicates increased to 30% ($n = 18$), consistent with decreased sample stability observed over longer time periods.

Method replicates were conducted to evaluate the ability of the sample preparation process to yield comparable measurements for samples made from the same original sediment. The reproducibility of method replicates also is controlled by variability within the sediment sample, and thus controlled by homogenization of the samples. We calculate an average RPD of 14% ($n = 35$) and 19% ($n = 27$) for method replicates from Lake El'Gygytgyn and Island Lake, respectively. This low error indicates sufficient sample homogenization and high reproducibility of the rBC measurement for samples prepared using this method. As standard protocol, we recommend preparing a small number of method replicates to evaluate measurement consistency both within and between runs.

Sample homogenization also controlled reproducibility and recovery of the rBC measurements, with inadequate homogenization resulting in weaker method reproducibility and lower rBC recovery. Various homogenization methods were tested using a bulk sediment sample from Island Lake. Groups of samples were prepared with (1) no homogenization, (2) mortar

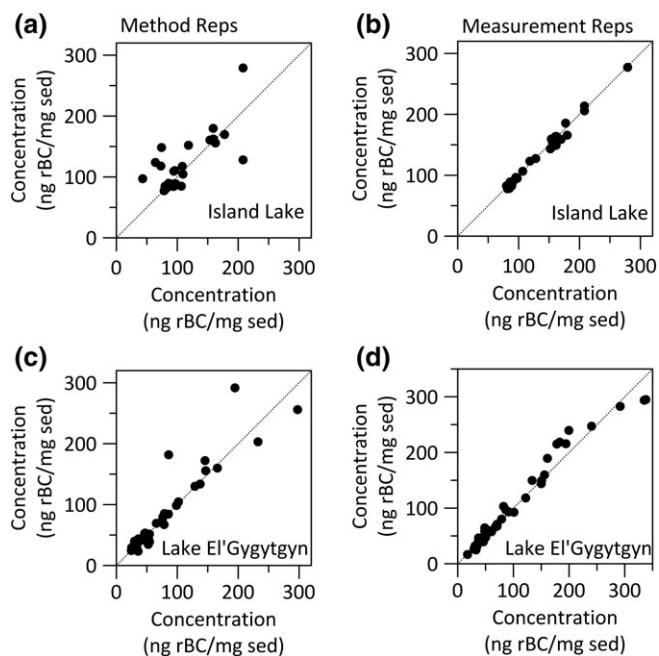


Fig. 5. Repeated measurements of samples from Island Lake (a,b) and Lake El'Gygytgyn (c,d) show that both method (left) and measurement (right) replicates were highly reproducible. 1 : 1 line plotted for reference.

and pestle grinding by hand, and (3) milling in a planetary ball mill for 1, 5, 10, and 20 min.

rBC concentration for Island Lake samples that had not been homogenized, ground with the mortar and pestle, or milled for one minute had ~ 25% lower concentrations than the samples that had been milled for 5, 10, and 20 min, indicating under-recovery. The average coefficient of variation (CV) of the rBC concentration for the groups that were not homogenized, ground by mortar and pestle, or milled for 1 and 5 min was 41%, 11%, 47%, and 31%, respectively ($n = 4$ for all groups). The CV for the samples ground by mortar and pestle was anomalously low. The CV declined to 11% and 8% for the groups milled for 10 and 20 min, respectively, indicating increased repeatability. Thus, 5 min of milling was required to achieve full rBC concentration, and the variability of the measurement declined with increased homogenization. rBC particle mass distributions were not significantly altered for milling times up to 20 min. Lake El'Gygytgyn samples were acquired after milling for 3 min. The low RPD for the Lake El'Gygytgyn replicate measurements indicates this was sufficient homogenization for these samples. We recommend homogenization with a ball mill for all sediments used with this method, with a milling time determined to yield sufficiently repeatable measurements.

Comparison to existing methods for BC analysis

To evaluate the new SP2-based measurement against an existing method, we captured the dry aerosol generated from the sediment samples on quartz-fiber filters to measure BC using the well-established IMPROVE_A method for carbon analysis (Chow et al. 2007). The IMPROVE_A method and other variations of it have been used extensively for long-term atmospheric measurements as well as lake sediment measurements (Chow et al. 2007; Han et al. 2007; Han et al. 2011). In

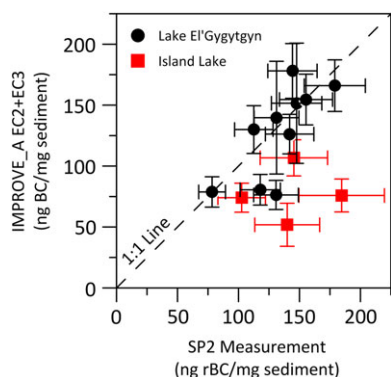


Fig. 6. Comparison of independent SP2 and IMPROVE_A (EC2 + EC3 fractions) measurements of BC for Lake El'Gygytgyn ($n = 10$) and Island Lake ($n = 4$) samples. Vertical error bars represent uncertainties from the IMPROVE_A method derived from replicate analyses and the minimum detection limit (Chow et al. 2007). Horizontal error bars represent the relative percentage difference of method replicates from the SP2 measurements. The IMPROVE_A method underestimated BC relative to SP2 measurements at island Lake.

short, a quartz-fiber filter was installed downstream of the Apex-Q to intercept the dry aerosol that normally would be sent to the SP2 (Fig. 1, location denoted by dashed arrow). Additional air flow of 3.5 L/min was added immediately prior to the filter to ensure uniform aerosol deposition on the filter and outflow from the filter was routed to the SP2 to verify 100% filtration efficiency. The dry aerosol was filtered for 40–60 min to ensure sufficient BC deposition to meet or exceed the detection limit of ~ 1500 μg BC/filter required for the IMPROVE_A method. Both before installing and after removing the filter, the aerosol was routed to the SP2 to determine an average SP2-predicted rBC loading on each filter.

After sampling, a 0.5-cm² punch was taken from the filter and inserted into a heating chamber where the temperature was increased in seven sequential steps from 150°C to 800°C under nonoxidizing conditions (100% helium atmosphere from 150°C to 550°C) and oxidizing conditions (90% helium, 2% oxygen from 550°C to 800°C) following standard IMPROVE-A protocols. During the stepwise combustion, different fractions of carbon were pyrolyzed to CO₂ and subsequently reduced to CH₄ which was then quantified by a flame-ionization detector. Elemental carbon was pyrolyzed in three heating steps under oxidizing conditions, with the total carbon pyrolyzed at each step referred to as EC1, EC2, and EC3. We considered the sum of the carbon measured during the oxidized heating phases at 700 and 800 °C, referred to as EC2 and EC3 fractions in the IMPROVE_A protocol, as the soot BC (Han et al. 2007; Han et al. 2011) and therefore most similar to the rBC detected by the SP2. EC1, referred to as char BC, generally is thought to be larger in size than the smaller, more refractory soot component (Han et al. 2011). It is possible, however, that the SP2 is sensitive to certain components of the EC1 fraction depending on the morphology. Previous studies have shown that atmospheric SP2 measurements were directly comparable to total EC as determined by filter-based thermal-optical methods that were unable to distinguish between EC1, EC2, and EC3 (Kondo et al. 2011; Laborde et al. 2013). Because the SP2 is most sensitive to rBC, we note that a comparison to the CTO-375 method that also only detects the soot rBC (Elmqvist et al. 2006) would be valuable for future work.

The results of this method intercomparison (Fig. 6) showed that for Lake El'Gygytgyn, most of the SP2 and EC2 + EC3 IMPROVE_A measurements agree within their uncertainties. The RPD between the two methods was 15% ($n = 10$), lending high confidence to the SP2 rBC determinations at Lake El'Gygytgyn. The strong agreement between methods at Lake El'Gygytgyn indicate that there are minimal or no sediment interferences on the SP2 measurement and the EC2 + EC3 soot BC is comparable to SP2-detected rBC at this site.

For Island Lake, the two methods had a RPD of 59% ($n = 4$), though only four samples were tested. The EC2 + EC3 portion of the IMPROVE_A method underestimated the BC concentration of the Island Lake samples relative to the SP2

rBC measurement, a discrepancy that could result from discounting the EC1 fraction of the IMPROVE_A method. Perhaps at this site, the SP2 is more sensitive to char BC associated with the EC1 fraction because of differing BC morphologies. However, the small number of measurements ($n = 4$) prevents conclusive evaluation for Island Lake samples.

Furthermore, observed concentrations for Lake El'Gygytgyn and Island Lake samples measured using the SP2 range from 100 to 300 ng rBC per mg sediment. The magnitude of these values is comparable to BC concentrations reported for lakes in northern Europe of 600–5100 ng BC per mg sediment using the soot-sensitive CTO-375 method (Ruppel et al. 2015) and 100–900 ng BC per mg sediment (calculated as EC2 + EC3) in China using the TOR method (Han et al. 2011).

To place measurements of environmental samples made using this new method into context with existing methods, we analyzed standard reference materials (SRMs), similar to Hammes et al. (2007) that compared seven methods for measuring BC in soils and sediments. We measured three SRMs from the National Institute of Standards and Technology, Urban Aerosol SRM 1648a, Marine Sediment SRM 2703, and Bituminous Coal SRM 1632c. These are not identical to the SRMs used in Hammes et al. (2007) but are similar enough to indicate if the new method generally agrees with existing methods. It is important to note that there are no SRMs certified for BC, so while analysis of SRMs is valuable to contextualize measurements made using methods, this approach cannot assess which method is the most accurate.

For the Urban Aerosol SRM 1648a, the SP2 method returned a measurement of 11 g rBC per kg, comparable to the range of 7–100 g BC per kg reported in Hammes et al. (2007) for SRM 1649a. For the Marine Sediment, the SP2 method returned a measurement of 1.9 g rBC per kg, comparable to the range of 0.9–11 g BC per kg for SRM 1941b. The SP2 was insensitive to bituminous coal (0.2 g rBC per kg), confirming that it is insensitive to nonpyrogenic carbon in this matrix.

Sample size

The high sensitivity of the SP2 allows for robust rBC measurements with small sediment sample requirements. Limitations on sample size are not limited by the SP2 detection limit, which at 2.1 ng/g is far below the observed rBC concentrations at Island Lake, Lake El'Gygytgyn, and other reported lakes (Han et al. 2011; Ruppel et al. 2015). As standard protocol, we use a sediment-to-water ratio of 1 mg sediment per 1 mL of water. To determine whether the rBC measurement scales 1 : 1 with sediment amount used, we tested samples prepared with sediment-to-water ratios ranging from 0.3 to 3 mg sediment per ml water for Lake El'Gygytgyn samples and from 0.3 to 1 mg sediment per ml water for Island Lake samples. All samples were prepared in 50 mL water by varying the amount of sediment.

rBC concentration showed no significant difference relative to the sediment-to-water ratio of 1 mg sediment per ml water at the 95% confidence interval using Student's t test for either set of samples, indicating it is possible to get reliable concentration measurements with as little as 15 mg of sediment. However, we recommend a samples size of 50 mg to minimize errors from the weighing process, for a better representation of the larger sample, and to reduce the need for further downstream dilution compared to larger samples. With the low sample requirement, resolution of rBC measurements in lake sediment cores with this method are generally limited more by the resolution of subsampling of the core than by sample size requirements.

Comments and recommendations

This method is a significant advance for BC research as it can be used to rapidly develop regional records of rBC deposition from lakes, which unlike ice cores, are geographically widespread across the globe. Such records provide important constraints for modeled rBC deposition (Lee et al. 2013) and for understanding rBC climate forcing, based on the assumption that rBC deposited in lake sediments is directly representative of atmospheric rBC. To develop valid rBC records that represent an atmospheric signal, significant consideration must be given to a lake's geographic setting and its depositional environment. For implementation of this method, we recommend the use of an SP2 capable of measuring the color ratio to quantify iron oxide interferences, and a thorough evaluation of the SP2-based method at each lake to ensure that sediment matrix effects and potential suspended sediment interferences are minimal. This study has shown that for Lake El'Gygytgyn and Island Lake, there are no particle interferences from sediment as small as 2 μm diameter and the sediment matrix does not adversely affect measurement of synthetic rBC standards in spiked samples. We suggest using the color ratio of samples to quantify and correct for interferences from particles smaller than 2 μm and in the same size range as rBC. Conducting a comparison to the IMPROVE_A or CTO-375 method with a select set of representative samples from a given lake record is valuable for evaluating the efficacy of the method for lake sediments with different mineralogies. Further validation and assessment of the SP2 method is required before it can be used independently of other well-established methods. For Island Lake and Lake El'Gygytgyn, this method was shown to provide a relatively rapid and robust approach for quantifying rBC.

References

- Arienzo, M. M., J. R. McConnell, L. N. Murphy, N. Chellman, S. Das, S. Kipfstuhl, and R. Mulvaney. 2017. Holocene black carbon in Antarctica paralleled southern hemisphere climate. *J. Geophys. Res. Atmos.* **122**: 6713–6728. doi: [10.1002/2017jd026599](https://doi.org/10.1002/2017jd026599)

- Augustin, L. and others. 2004. Eight glacial cycles from an Antarctic ice core. *Nature* **429**: 623–628. doi:[10.1038/nature02599](https://doi.org/10.1038/nature02599)
- Bauer, S. E., A. Bausch, L. Nazarenko, K. Tsigaridis, B. Xu, R. Edwards, M. Bisiaux, and J. McConnell. 2013. Historical and future black carbon deposition on the three ice caps: Ice core measurements and model simulations from 1850 to 2100. *J. Geophys. Res.-Atmos.* **118**: 7948–7961. doi:[10.1002/jgrd.50612](https://doi.org/10.1002/jgrd.50612)
- Baumgardner, D. and others. 2012. Soot reference materials for instrument calibration and intercomparisons: A workshop summary with recommendations. *Atmos. Meas. Tech.* **5**: 1869–1887. doi:[10.5194/amt-5-1869-2012](https://doi.org/10.5194/amt-5-1869-2012)
- Bisiaux, M. M., R. Edwards, J. R. McConnell, M. R. Albert, H. Anschutz, T. A. Neumann, E. Isaksson, and J. E. Penner. 2012. Variability of black carbon deposition to the East Antarctic plateau, 1800–2000 AD. *Atmos. Chem. Phys.* **12**: 3799–3808. doi:[10.5194/acp-12-3799-2012](https://doi.org/10.5194/acp-12-3799-2012)
- Bisiaux, M. M. and others. 2012. Changes in black carbon deposition to Antarctica from two high-resolution ice core records, 1850–2000 AD. *Atmos. Chem. Phys.* **12**: 4107–4115. doi:[10.5194/acp-12-4107-2012](https://doi.org/10.5194/acp-12-4107-2012)
- Bond, T. C. and others. 2013. Bounding the role of black carbon in the climate system: A scientific assessment. *J. Geophys. Res. Atmos.* **118**: 5380–5552. doi:[10.1002/jgrd.50171](https://doi.org/10.1002/jgrd.50171)
- Brigham-Grette, J. and others. 2013. Pliocene warmth, polar amplification, and stepped Pleistocene cooling recorded in NE Arctic Russia. *Science* **340**: 1421–1427. doi:[10.1126/science.1233137](https://doi.org/10.1126/science.1233137)
- Chellman, N., J. R. McConnell, M. Arienzo, G. T. Pederson, S. M. Aarons, and A. Csank. 2017. Reassessment of the upper Fremont glacier ice-Core chronologies by synchronizing of ice-Core-water isotopes to a nearby tree-ring chronology. *Environ. Sci. Technol.* **51**: 4230–4238. doi:[10.1021/acs.est.6b06574](https://doi.org/10.1021/acs.est.6b06574)
- Chow, J. C., J. G. Watson, L. W. A. Chen, M. C. O. Chang, N. F. Robinson, D. Trimble, and S. Kohl. 2007. The IMPROVE-A temperature protocol for thermal/optical carbon analysis: Maintaining consistency with a long-term database. *J. Air Waste Manage. Assoc.* **57**: 1014–1023. doi:[10.3155/1047-3289.57.9.1014](https://doi.org/10.3155/1047-3289.57.9.1014)
- Dahl-Jensen, D. and others. 2013. Eemian interglacial reconstructed from a Greenland folded ice core. *Nature* **493**: 489–494. doi:[10.1038/nature11789](https://doi.org/10.1038/nature11789)
- Elmquist, M., G. Cornelissen, Z. Kukulska, and Ö. Gustafsson. 2006. Distinct oxidative stabilities of char versus soot black carbon: Implications for quantification and environmental recalcitrance. *Global Biogeochem. Cycle* **20**: GB2009. doi:[10.1029/2005GB002629](https://doi.org/10.1029/2005GB002629)
- Gustafsson, O., T. D. Bucheli, Z. Kukulska, M. Andersson, C. Largeau, J. N. Rouzaud, C. M. Reddy, and T. I. Eglinton. 2001. Evaluation of a protocol for the quantification of black carbon in sediments. *Global Biogeochem. Cycle* **15**: 881–890. doi:[10.1029/2000gb001380](https://doi.org/10.1029/2000gb001380)
- Gysel, M., M. Laborde, J. S. Olfert, R. Subramanian, and A. J. Groehn. 2011. Effective density of Aquadag and fullerene soot black carbon reference materials used for SP2 calibration. *Atmos. Meas. Tech.* **4**: 2851–2858. doi:[10.5194/amt-4-2851-2011](https://doi.org/10.5194/amt-4-2851-2011)
- Hammes, K. and others. 2007. Comparison of quantification methods to measure fire-derived (black/elemental) carbon in soils and sediments using reference materials from soil, water, sediment and the atmosphere. *Global Biogeochem. Cycle* **21**: GB3016. doi:[10.1029/2006gb002914](https://doi.org/10.1029/2006gb002914)
- Han, Y. M., J. J. Cao, B. Z. Yan, T. C. Kenna, Z. D. Jin, Y. Cheng, J. C. Chow, and Z. S. An. 2011. Comparison of elemental carbon in Lake sediments measured by three different methods and 150-year pollution history in eastern China. *Environ. Sci. Technol.* **45**: 5287–5293. doi:[10.1021/es103518c](https://doi.org/10.1021/es103518c)
- Han, Y. N., J. J. Cao, Z. S. An, J. C. Chow, J. G. Watson, Z. Jin, K. Fung, and S. X. Liu. 2007. Evaluation of the thermal/optical reflectance method for quantification of elemental carbon in sediments. *Chemosphere* **69**: 526–533. doi:[10.1016/j.chemosphere.2007.03.035](https://doi.org/10.1016/j.chemosphere.2007.03.035)
- Kaspari, S. D., M. Schwikowski, M. Gysel, M. G. Flanner, S. Kang, S. Hou, and P. A. Mayewski. 2011. Recent increase in black carbon concentrations from a Mt. Everest ice core spanning 1860–2000 AD. *Geophys. Res. Lett.* **38**: L04703. doi:[10.1029/2010gl046096](https://doi.org/10.1029/2010gl046096)
- Keegan, K. M., M. R. Albert, J. R. McConnell, and I. Baker. 2014. Climate change and forest fires synergistically drive widespread melt events of the Greenland ice sheet. *Proc. Natl. Acad. Sci. USA* **111**: 7964–7967. doi:[10.1073/pnas.1405397111](https://doi.org/10.1073/pnas.1405397111)
- Khan, A. J., K. Swami, T. Ahmed, A. Bari, A. Shareef, and L. Husain. 2009. Determination of elemental carbon in lake sediments using a thermal-optical transmittance (TOT) method. *Atmos. Environ.* **43**: 5989–5995. doi:[10.1016/j.atmosenv.2009.08.030](https://doi.org/10.1016/j.atmosenv.2009.08.030)
- Kondo, Y., L. Saho, N. Moteki, F. Khan, N. Takegawa, X. Liu, M. Koike, and T. Miyakawa. 2011. Consistency and traceability of black carbon measurements made by laser-induced incandescence, thermal-optical transmittance, and filter-based photo-absorption techniques. *Aerosol Sci. Tech.* **45**: 295–312. doi:[10.1080/02786826.2010.533215](https://doi.org/10.1080/02786826.2010.533215)
- Laborde, M., P. Mertes, P. Zieger, J. Dommén, U. Baltensperger, and M. Gysel. 2012. Sensitivity of the single particle soot photometer to different black carbon types. *Atmos. Meas. Tech.* **5**: 1031–1043. doi:[10.5194/amt-5-1031-2012](https://doi.org/10.5194/amt-5-1031-2012)
- Laborde, M. and others. 2013. Black carbon physical properties and mixing state in the European megacity Paris. *Atmos. Chem. Phys.* **13**: 5831–5856. doi:[10.5194/acp-13-5831-2013](https://doi.org/10.5194/acp-13-5831-2013)
- Lee, Y. H. and others. 2013. Evaluation of preindustrial to present-day black carbon and its albedo forcing from atmospheric chemistry and climate model Intercomparison project (ACCMIP) (vol 13, pg 2607, 2013). *Atmos. Chem. Phys.* **13**: 6553–6554. doi:[10.5194/acp-13-6553-2013](https://doi.org/10.5194/acp-13-6553-2013)
- Louchouart, P. and others. 2007. Elemental and molecular evidence of soot- and char-derived black carbon inputs to

- New York City's Atmos. During the 20th century. *Environ. Sci. Technol.* **41**: 82–87. doi:[10.1021/es061304+](https://doi.org/10.1021/es061304+)
- MacDonald, K. M. and others. 2017. Observations of atmospheric chemical deposition to high Arctic snow. *Atmos. Chem. Phys.* **17**: 5775–5788. doi:[10.5194/acp-17-5775-2017](https://doi.org/10.5194/acp-17-5775-2017)
- Marlon, J. R., P. J. Bartlein, C. Carcaillet, D. G. Gavin, S. P. Harrison, P. E. Higuera, F. Joos, M. J. Power, and I. C. Prentice. 2008. Climate and human influences on global biomass burning over the past two millennia. *Nat. Geosci.* **1**: 697–702. doi:[10.1038/ngeo313](https://doi.org/10.1038/ngeo313)
- McConnell, J. R., and R. Edwards. 2008. Coal burning leaves toxic heavy metal legacy in the Arctic. *Proc. Natl. Acad. Sci. USA* **105**: 12140–12144. doi:[10.1073/pnas.0803564105](https://doi.org/10.1073/pnas.0803564105)
- McConnell, J. R. and others. 2007. 20th-century industrial black carbon emissions altered arctic climate forcing. *Science* **317**: 1381–1384. doi:[10.1126/science.1144856](https://doi.org/10.1126/science.1144856)
- Melles, M., J. Brigham-Grette, O. Y. Glushkova, P. S. Minyuk, N. R. Nowaczyk, and H.-W. Hubberten. 2007. Sedimentary geochemistry of core PG1351 from Lake El'gygytgyn—a sensitive record of climate variability in the east Siberian Arctic during the past three glacial-interglacial cycles. *J. Paleolimnol.* **37**: 89–104. doi:[10.1007/s10933-006-9025-6](https://doi.org/10.1007/s10933-006-9025-6)
- Melles, M. and others. 2012. 2.8 million years of Arctic climate change from Lake El'gygytgyn, NE Russia. *Science* **337**: 315–320. doi:[10.1126/science.1222135](https://doi.org/10.1126/science.1222135)
- Moteki, N. and others. 2007. Evolution of mixing state of black carbon particles: Aircraft measurements over the western Pacific in March 2004. *Geophys. Res. Lett.* **34**: L11803. doi:[10.1029/2006GL028943](https://doi.org/10.1029/2006GL028943)
- Muri, G., B. Cermelj, J. Faganeli, and J. Holc. 2002. Determination of black carbon in lacustrine and coastal marine sediments by thermal oxidation. *Acta Chim. Slov.* **49**: 29–42.
- Ohata, S., N. Moteki, J. Schwarz, D. Fahey, and Y. Kondo. 2013. Evaluation of a method to measure black carbon particles suspended in rainwater and snow samples. *Aerosol Sci. Tech.* **47**: 1073–1082. doi:[10.1080/02786826.2013.824067](https://doi.org/10.1080/02786826.2013.824067)
- Painter, T. H., M. G. Flanner, G. Kaser, B. Marzeion, R. A. VanCuren, and W. Abdalati. 2013. End of the little ice age in the Alps forced by industrial black carbon. *Proc. Natl. Acad. Sci. USA* **110**: 15216–15221. doi:[10.1073/pnas.1302570110](https://doi.org/10.1073/pnas.1302570110)
- Petzold, A. and others. 2013. Recommendations for reporting “black carbon” measurements. *Atmos. Chem. Phys.* **13**: 8365–8379. doi:[10.5194/acp-13-8365-2013](https://doi.org/10.5194/acp-13-8365-2013)
- Ruppel, M. M. and others. 2015. Spatial and temporal patterns in black carbon deposition to dated Fennoscandian Arctic Lake sediments from 1830 to 2010. *Environ. Sci. Tech.* **49**: 13954–13963. doi:[10.1021/acs.est.5b01779](https://doi.org/10.1021/acs.est.5b01779)
- Schwarz, J. P. and others. 2006. Single-particle measurements of midlatitude black carbon and light-scattering aerosols from the boundary layer to the lower stratosphere. *J. Geophys. Res. Atmos.* **111**: D16207. doi:[10.1029/2006JD007076](https://doi.org/10.1029/2006JD007076)
- Schwarz, J. P. and others. 2010. The detection efficiency of the single particle soot photometer. *Aerosol Sci. Tech.* **44**: 612–628. doi:[10.1080/02786826.2010.481298](https://doi.org/10.1080/02786826.2010.481298)
- Schwarz, J. P., R. S. Gao, A. E. Perring, J. R. Spackman, and D. W. Fahey. 2013. Black carbon aerosol size in snow. *Sci. Rep.* **3**: 1–5. doi:[10.1038/srep01356](https://doi.org/10.1038/srep01356)
- Subramanian, R. and others. 2010. Black carbon over Mexico: The effect of atmospheric transport on mixing state, mass absorption cross-section, and BC/CO ratios. *Atmos. Chem. Phys.* **10**: 219–237. doi:[10.5194/acp-10-219-2010](https://doi.org/10.5194/acp-10-219-2010)
- Vanni re, B., D. Colombaroli, E. Chapron, A. Leroux, W. Tinner, and M. Magny. 2008. Climate versus human-driven fire regimes in Mediterranean landscapes: The Holocene record of Lago dell'Accesa (Tuscany, Italy). *Quat. Sci. Rev.* **27**: 1181–1196. doi:[10.1016/j.quascirev.2008.02.011](https://doi.org/10.1016/j.quascirev.2008.02.011)
- Vanni re, B. and others. 2011. Circum-Mediterranean fire activity and climate changes during the mid-Holocene environmental transition (8500–2500 cal. BP). *Holocene* **21**: 53–73. doi:[10.1177/0959683610384164](https://doi.org/10.1177/0959683610384164)
- Vanni re, B. and others. 2016. 7000-year human legacy of elevation-dependent European fire regimes. *Quat. Sci. Rev.* **132**: 206–212. doi:[10.1016/j.quascirev.2015.11.012](https://doi.org/10.1016/j.quascirev.2015.11.012)
- Wendl, I. A., J. A. Menking, R. Faerber, M. Gysel, S. D. Kaspari, M. J. G. Laborde, and M. Schwikowski. 2014. Optimized method for black carbon analysis in ice and snow using the single particle soot photometer. *Atmos. Meas. Tech.* **7**: 2667–2681. doi:[10.5194/amt-7-2667-2014](https://doi.org/10.5194/amt-7-2667-2014)
- Whitlock, C., and S. H. Millspaugh. 1996. Testing the assumptions of fire history studies: An examination of modern charcoal accumulation in Yellowstone National Park, USA. *Holocene* **6**: 7–15. doi:[10.1177/095968369600600102](https://doi.org/10.1177/095968369600600102)
- Yang, H., and J. Z. Yu. 2002. Uncertainties in charring correction in the analysis of elemental and organic carbon in atmospheric particles by thermal/optical methods. *Environ. Sci. Technol.* **36**: 5199–5204. doi:[10.1021/es025672z](https://doi.org/10.1021/es025672z)
- Yoshida, A., N. Moteki, S. Ohata, T. Mori, R. Tada, P. Dagsson-Waldhauserova, and Y. Kondo. 2016. Detection of light-absorbing iron oxide particles using a modified single-particle soot photometer. *Aerosol Sci. Tech.* **50**: 1–4. doi:[10.1080/02786826.2016.1146402](https://doi.org/10.1080/02786826.2016.1146402)
- Zennaro, P. and others. 2014. Fire in ice: Two millennia of boreal forest fire history from the Greenland NEM ice core. *Clim. Past* **10**: 1905–1924. doi:[10.5194/cp-10-1905-2014](https://doi.org/10.5194/cp-10-1905-2014)

Acknowledgments

The authors would like to acknowledge the Sulo and Aileen Maki Endowment at DRI for funding this research. The authors thank P. Minyuk, G. Federov, G. Schwamborn, M. A. Haker, O. Juschus, and S. Quart for their help in recovering the sediment core from Lake El'Gygytgyn in 2003. The authors thank J. Stone and S. Brown for providing samples from Island Lake. The authors also thank the X. Wang and the Environmental Analysis Facility at DRI for the IMPROVE_A analysis and H. Moosm ller and A. Khlystov for lending their DMA for SP2 calibration. The authors thank the two reviewers for their insightful comments. This work has been possible with support from Region Franche-Comt  (France), the CNRS PaleoMex-MISTRALS project, and Pole 2 of the MSHE. Collaboration among the scientists involved in this

study resulted from networking within the PAGES Global Paleofire Working Group and was initiated as a result of the 2013 workshop held in Venice, Italy.

Submitted 8 May 2018
Revised 22 August 2018
Accepted 27 August 2018

Conflict of Interest

None declared.

Associate editor: John Smol